Fluorene functionalised sexithiophenes—utilising intramolecular charge transfer to extend the photocurrent spectrum in organic solar cells†

Peter J. Skabara,*[a] Rory Berridge,[b] Igor M. Serebryakov,‡[b] Alexander L. Kanibolotsky,[a] Lyudmila Kanibolotskaya,[a] Sergey Gordeyev,[a] Igor F. Perepichka,§*[c] N. Serdar Sariciftci*[d] and Christoph Winder[d]

Received 11th July 2006, Accepted 28th November 2006
First published as an Advance Article on the web 14th December 2006
DOI: 10.1039/b609858d

A new series of oligothiophenes bearing electron deficient fluorene units have been prepared and characterised. The materials are functionalised by C_8/C_{11} alkyl chains or triethylene glycol side groups, yet the higher oligomers remain poorly soluble. The absorption characteristics of a sexithiophene analogue (compound **3**) have been studied by UV-vis and photoinduced absorption spectroscopy. Photovoltaic cells have been fabricated from blends of **3** and fullerene derivative [6,6]-phenyl-C_{61} butyric acid methyl ester (PCBM). The photocurrent spectrum of the device matches the absorption spectrum of the sexithiophene system which incorporates an intramolecular charge transfer band arising from the 1,3-dithiole-fluorene units. A modest power conversion efficiency of 0.1% was achieved.

Introduction

Polythiophenes and well-defined oligothiophenes have been investigated as organic semiconductor materials for application in various electronic devices, such as organic photovoltaic cells (OPVs),[1–4] light emitting diodes and electrochromics,[5–8] and organic field effect transistors.[9–12] In OPVs, π-electron rich conjugated systems are either blended or tethered to electron acceptor molecules and, almost exclusively, the latter are derivatives of the fullerene C_{60}.[13] Photoexcitation of the organic material(s) generates a charge separated state which, under constrained device parameters, allows the generation of a potential difference across the OPV device.

We have previously reported the synthesis of a series of thiophene[14] and terthiophene[15,16] monomers bearing substituted fluorene units. The substituents vary in number and in their electron withdrawing strength (nitro and ester functionalities were applied). Intramolecular charge transfer (ICT) between fluorene and 1,3-dithiole units is a common feature in these materials and we found a Hammett-type dependence between the sum of the nucleophilic constants of the substituents and ICT energies. The same relationship was identified for the values of the first two reduction processes of the compounds, which are features of the fluorene units. Electropolymerisation of a trinitro analogue of the terthiophene series gave polymer **1**.[16] Photoinduced IR spectroscopy of this polymer showed evidence of a long lived charge separated state, indicating that the material could be a good candidate for OPVs. However, even though the repeat unit is furnished with a triethylene glycol chain, this functionality is not sufficient to impart good solubility to the polymer, which is an obvious problem towards processing the material. To this end, we decided to turn our attention towards the synthesis of oligomeric analogues, which are soluble in common organic solvents and can be processed by standard and cheap solution based techniques. Herein, we report the synthesis and characterisation of compounds **2** and **3** and the application of the latter in an OPV device.

Synthesis

In the search for more soluble materials, the most obvious option was to increase the number of long-chain substituents in the fluorene moiety whilst retaining strong acceptor ability. In line with this, we chose to investigate comparatively easily accessible fluorene derivatives, namely diesters of fluorene-2,7-dicarboxylic acid and 2,7-dialkylsulfonyl fluorenes. Each of the series was prepared in two modifications, either with a long (C_{11} or C_8) n-alkyl substituent or with a triethylene glycol monomethyl ether chain which should favour solubility of the compounds in correspondingly low- and high-polar solvents.

Fluorene-2,7-dicarboxylic acid and its diesters

Apart from the known procedures of direct carboxylation of fluorene,[17,18] for which the isomeric purity of products had not been assessed, a promising option was the conversion of 2,7-diacetylfluorene **4**, which, in our experience, could be easily

[a] *WestCHEM, Department of Pure and Applied Chemistry, University of Strathclyde, 295, Cathedral Street, Glasgow, UK G1 1XL. E-mail: peter.skabara@strath.ac.uk; Fax: +44 141 548 4822; Tel: +44 141 548 4648*
[b] *School of Chemistry, University of Manchester, Oxford Road, Manchester, UK M13 9PL*
[c] *L. M. Litvinenko Institute of Physical Organic and Coal Chemistry, National Academy of Sciences of Ukraine, Donetsk 83114, Ukraine*
[d] *Linz Institute for Organic Solar Cells (LIOS), Physical Chemistry, Johannes Kepler University Linz, Linz A-4040, Austria. E-mail: Serdar.Sariciftci@jk.uni-linz.ac.at*
† Electronic supplementary information (ESI) available: experimental and analytical data for all new compounds, details of CV and SEC experiments. See DOI: 10.1039/b609858d
‡ Present Address: Department of Organic Chemistry, Donetsk National University, Donetsk 83055, Ukraine.
§ Currently at: Department of Chemistry, Durham University, Durham, UK DH1 3LE. E-mail: i.f.perepichka@durham.ac.uk.

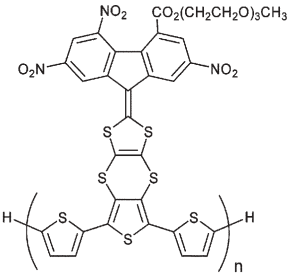

1

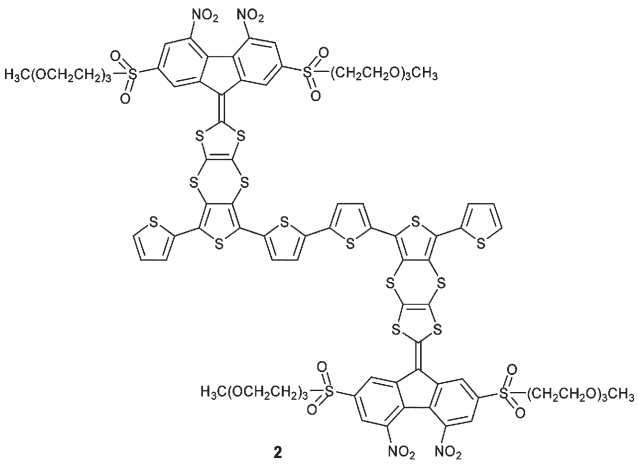

2

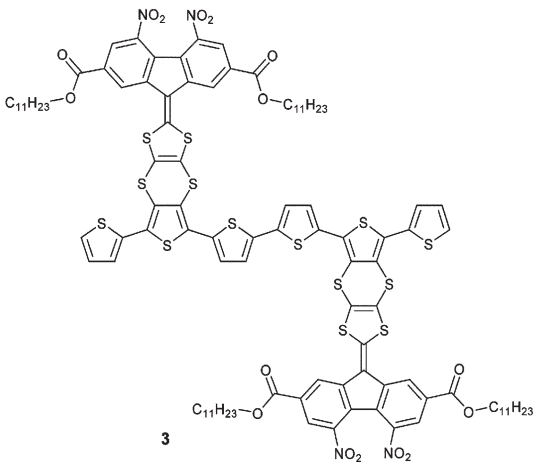

3

obtained and purified. Its oxidation furnished fluorenone-2,7-dicarboxylic acid[19] in high yield. However, in our hands, subsequent reduction of this intermediate with hydrazine hydrate in ethylene glycol[20] failed to yield the target product. Possibly, the use of a higher boiling solvent such as diethylene glycol[21] could afford the desired result but we did not explore this route any further.

The conversion of acetylfluorenes into the corresponding carboxylic acids, without simultneous oxidation of the methylene group, could be achieved in two ways. Coupling of 2,7-diacetylfluorene **4** with diethyl oxalate, followed by cleavage of the resulting bis-diketoester with lead tetraacetate, is known to give only moderate yield (33%) of fluorene-2,7-dicarboxylic acid.[22] A number of substituted fluorene-carboxylic acids was obtained by haloformic cleavage of acetylfluorenes in excellent yields;[23,24] however, applied to 2,7-diacetylfluorene **4**, this procedure yielded fluorenone-2,7-dicarboxylic acid. Use of a milder base (sodium carbonate) instead of sodium hydroxide under the same conditions resulted in unchanged diacetylfluorene.

Another way of using the haloformic reaction was to prepare 2,7-bis(tribromoacetyl)fluorene in a separate stage before its cleavage. However, the procedure described for α,α,α-tribromoacetophenone[25] yielded only contaminated 2,7-bis(dibromoacetyl)fluorene **5** which could also be obtained in quantitative yield by bromination of 2,7-diacetylfluorene **4** with bromine in hot acetic acid (Scheme 1). This product, however, appeared much more reactive towards further bromination in aqueous dioxane–sodium carbonate solutions which, accompanied by fast destruction of the tribromo derivative,[26] allowed the isolation of the target fluorene-2,7-dicarboxylic acid **6** in almost quantitative yield.

Diesters of fluorene-2,7-dicarboxylic acid (**7a,b**) were synthesised by an analogous procedure to that described[16] for 2,5,7-trinitrofluorene-4-carboxylic acid (triethylene glycol monomethyl ether) ester. However, nitration of these compounds produced target products (**8a,b**) contaminated with, most probably, 4,6-isomers (13–30% depending on conditions, NMR evidence), and, in the case of diundecyl ester, the monosubstituted compound which was poorly soluble in the nitrating mixture. Although all admixtures could be removed to a desired extent (less than 3%) by repetitive recrystallisation, this rendered only moderate yields.

Nitration of free fluorene-2,7-dicarboxylic acid led to even more complex mixtures of products, from which the target compound could be isolated only in low yield (12%). Our attempt to obtain chloroanhydride from this product led to its decomposition, as was found for 2,5,7-trinitrofluorene-4-carboxylic acid.[16]

Fluorene-2,7-disulfones

The most straightforward route to the target compounds (Scheme 2) included the reduction of fluorene-2,7-disulfonyl chloride **9** into the corresponding dimercaptan, followed by its subsequent alkylation to give **10a,b** and oxidation of the resulting sulfides (**11a,b**). However, the only described[27] synthetic procedure for fluorene-2,7-dimercaptan produced, as it had been found, only a low yield of target compound along with insoluble solid, most probably polydisulfide. The same product was isolated from an attempt to obtain a protected derivative, as was described for 2-*S*-acetylthiofluorene.[28] Though the polydisulfide could be converted into mercaptan sodium salt[29] with subsequent alkylation, this procedure was found to be inferior to direct *in situ* alkylation of fluorene-2,7-dimercaptan after reduction of disulfonyl chloride **9** with lithium aluminium hydride (Scheme 2).

Oxidation of the sulfides (**10a,b**) to the corresponding sulfones (**11a,b**) with hydrogen peroxide in boiling acetic acid proceeded smoothly within five minutes, whereas refluxing over 2 hours, as was suggested for fluorenyl-2-methylsulfide,[30] gave a product heavily contaminated with the corresponding fluorenone derivative (MS evidence) and other unspecified products.

Nitration of sulfones **11a,b** to afford compounds **12a,b** was regioselective, due to the greater orientating power of the sulfonyl substituents compared to the carboxyl groups.

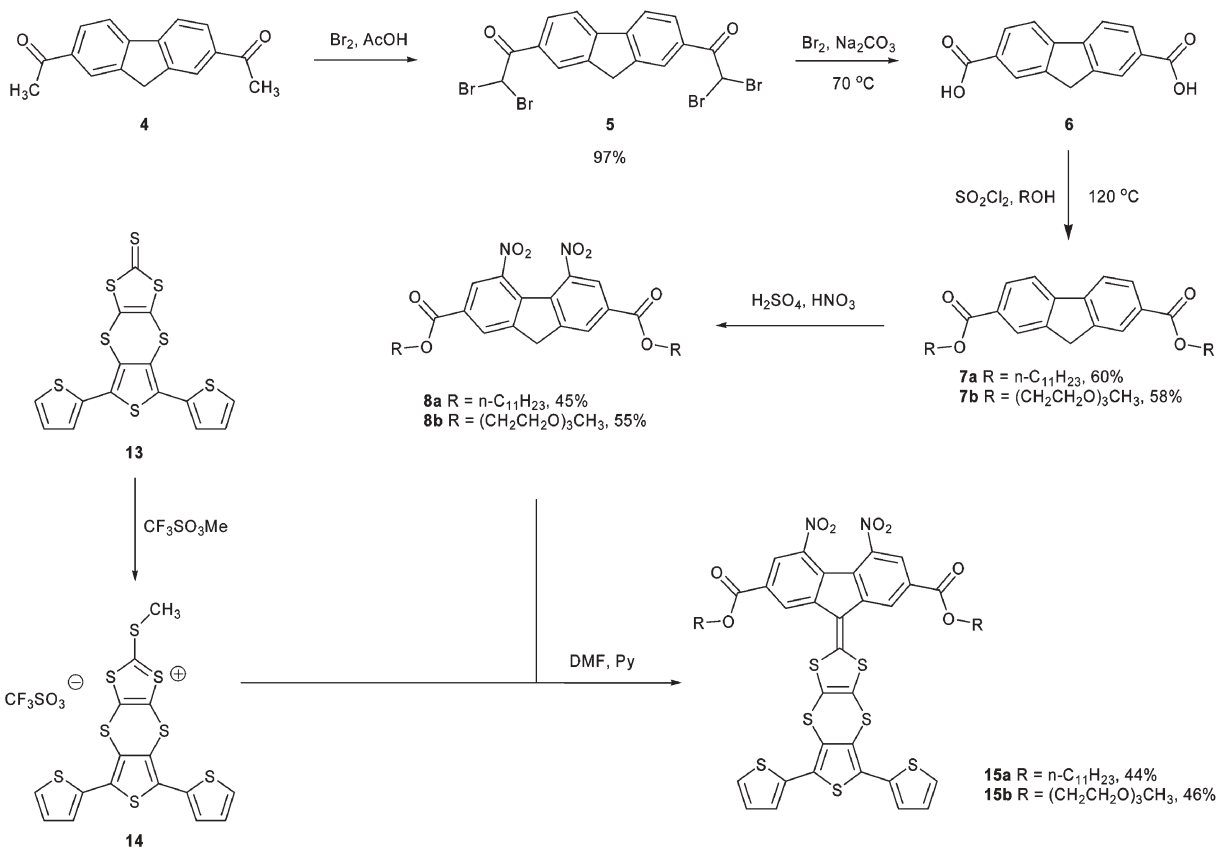

Scheme 1

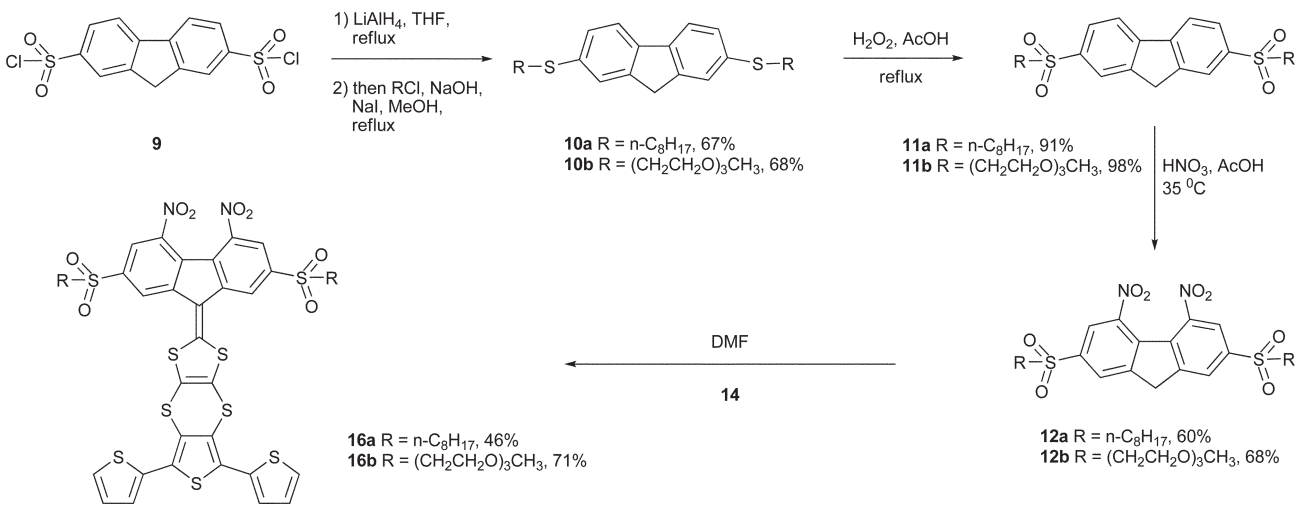

Scheme 2

However, the stronger electron withdrawing ability of the sulfonyl groups required more vigorous nitration conditions, in which the alkyl chains underwent attack by nitric acid to a substantial extent (NMR evidence). The resulting contaminants were removed by recrystallisation.

Coupling of the fluorene units **8a,b** and **12a,b** with terthiophene **13** (*via* the salt **14**) was achieved as described[16] in overall satisfactory yields. The coupling of disulfonyl derivatives **12a,b** proceeded smoothly in DMF, whereas the less reactive dicarbonyl compounds **8a,b** required addition of pyridine. Due to the poor solubility of fluorene-2,7-dicarboxylic acid diundecyl ester **8a** in DMF, the coupling was carried out in a DMF–chloroform mixture.

Chemical coupling of terthiophenes

As we have demonstrated previously,[15,16] terthiophene analogues of **15** and **16** can be polymerised electrochemically. This procedure is analogous to coupling using a chemical oxidant. In this part of the work, we chose to focus on the two most

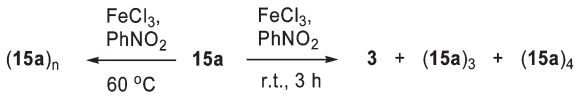

Scheme 3

soluble terthiophene derivatives, compounds **15a** and **16b**. Ferric chloride was added to solutions of the terthiophenes in nitrobenzene. At higher temperatures (up to 60 °C) and prolonged reaction times, we obtained polymeric material that was insoluble (after evaporation of the solvent) (Scheme 3). By performing the same reactions at room temperature for 3 hours we obtained mainly oligomeric material, but the isolated materials were adequately soluble in chlorinated solvents. MALDI-TOF mass spectrometry showed that the products were obtained as mixtures of oligomers (6T, 9T, 12T) and the main fraction from the reaction of **15a** (sexithiophene **3**, Scheme 3) was isolated by column chromatography to give a clean spectrum (see Fig. S1 in ESI†). For reasons of solubility and monodispersity, absorption and electrochemical studies, and device fabrication were performed only on compound **3**.

Electrochemistry and spectroelectrochemistry

Electrochemical studies of compound **3** were performed in benzonitrile solution using tetrabutylammonium hexafluorophosphate (Bu_4NPF_6) as supporting electrolyte and Ag/Ag^+ as reference electrode (0.01 M $AgNO_3$ in acetonitrile; potential +0.187 V *vs.* Fc/Fc^+ couple). Cyclic voltammetry experiments demonstrated electroactivity of **3** in both reduction and oxidation processes (Fig. 1). Reduction of compound **3** shows typical behaviour observed for electron acceptors of the fluorene series,[14,19,31,32] *i.e.* two consecutive single electron reduction waves resulting in a radical anion and dianion (on each fluorene moiety), respectively. In the case of **3**, the first reduction at $E_{1/2}^{red1} = -0.96$ V is almost a reversible process ($\Delta E_{pc\text{-}pa}^{red1} = 82$ mV), whereas the second reduction is electrochemically irreversible ($E_{pc}^{red2} = -1.35$ V; $\Delta E_{pc\text{-}pa}^{red2} \approx 200$ mV; $i_{pc} \gg i_{pa}$). Good reversibility of the first reduction wave indicates that both fluorene moieties are reduced at the same potential resulting in bis(radical anion) $\mathbf{3}^{2(\bullet-)}$ species, *i.e.* there is no electronic communication between the two fluorene units in compound **3**, as expected from its structure. Consequently, the second reduction wave represents the formation of bis(dianion) $\mathbf{3}^{4-}$. The difference of $\Delta E^{red1-2} \sim 0.35$ V between the first and second reduction processes is typical for fluorene acceptors ($\sim$0.3–0.5 V,[19,31] although fluorene acceptors with strong ICT show decreased ΔE^{red1-2} of $\sim$0.2 V[14,32]).

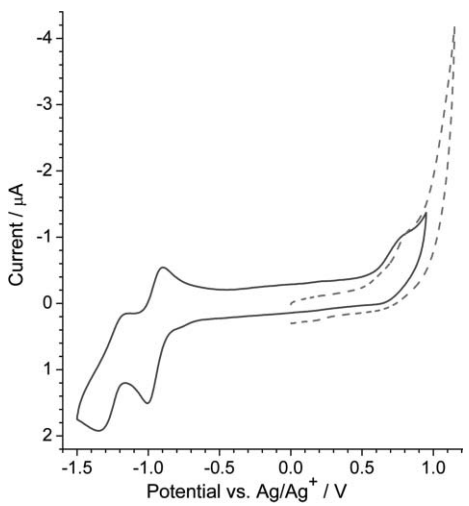

Fig. 1 Cyclic voltammetry of compound **3** in benzonitrile, 0.1 N Bu_4NPF_6; scan rate 100 mV s^{-1} (solid line: second cycle for reduction/oxidation; dashed line: oxidation up to +1.15 V).

Oxidation of compound **3** to the radical cation (as followed from the current i_{pa}^{ox1}, which is *ca.* twice as low as i_{pc}^{red1}) occurs as an electrochemically irreversible process with $E_{pa}^{ox1} \sim +0.8$ V *vs.* Ag/Ag^+ (Fig. 1) Obviously, E_{pa}^{ox1} corresponds to oxidation of the sexithiophene chain to produce a polaron state and this process is followed by further oxidation (presumably to a bipolaron state, which is complicated by the simultaneous oxidation of dithiole rings—in the case of 9-dithiolylidene-nitrofluorene acceptors the substrates are irreversibly oxidised above +1 V[14,16,32]). Cycling the potentials between 0 V and +1.2 V (as well as +1.4 V) did not show anodic electropolymerisation (or dimerisation) of **3**.

Spectroelectrochemical (SEC) experiments in benzonitrile solution were performed to establish the spectroscopic signatures of species generated in CV. In the neutral state, compound **3** has $\lambda_{max} = 439$ nm with two shoulders at 380 and 520 nm (in benzonitrile). On reduction of the fluorene units in **3** to radical anions (simultaneously on both fluorenes), the intensities of the peaks at 439 and 520 nm are increased and their maxima are slightly blue shifted (Fig. 2a). In addition, new broad absorption peaks appear in the long wavelength visible region (600–750 nm; isosbestic points at 530 and 580 nm) together with very low-intensity NIR absorption above 900 nm (Fig. 2a,c). Further reduction of the fluorene moieties to dianions results in a decrease of intensity for the peaks at $\sim$440–500 nm and in the NIR region (>900 nm), whereas the long wavelength visible absorption is broadened to $\sim$600–850 nm (Fig. 2a–c). Repeating the SEC experiment with $\sim$5 times higher concentration of **3** allowed the clear observation of NIR absorption of the fluorene radical anions on reduction of **3** (broad band at $\sim$900–1300 nm peaked at $\lambda_{max} = 1035$ nm and low intense shoulder at $\sim$1450 nm), which disappears on further reduction to the dianion species (Fig. 3). Such NIR absorption is characteristic for radical anions of fluorene electron acceptors and it was previously observed for electrochemically generated radical anions of polynitrofluorene derivatives, charge transfer complexes of fluorene acceptors with tetrathiafulvalene family donors, and ICT complexation in fluorene–σ-tetrathiafulvalene diads.[33,34]

Oxidation of compound **3** in the SEC experiment led to the observation of the radical cation at *ca.* +1.2 V (*vs.* Ag wire) by a slight decrease of intensity of the peak at 439 nm and an increase in the intensity of the shoulder at 520 nm (isosbestic point at $\sim$485 nm) (Fig. 4a). The radical cation $\mathbf{3}^{\bullet+}$ is also characterised by two new absorption bands: a long wavelength vis-NIR band at $\sim$650–900 nm and a broad low energy NIR absorbtion at >1200 nm (peaked at $\lambda_{max} = 1530$ nm) (Fig. 4a,c). Further increase of the potential results in a decrease of NIR absorption at 1530 nm, indicating further oxidative transformations of the $\mathbf{3}^{\bullet+}$ species (more detailed

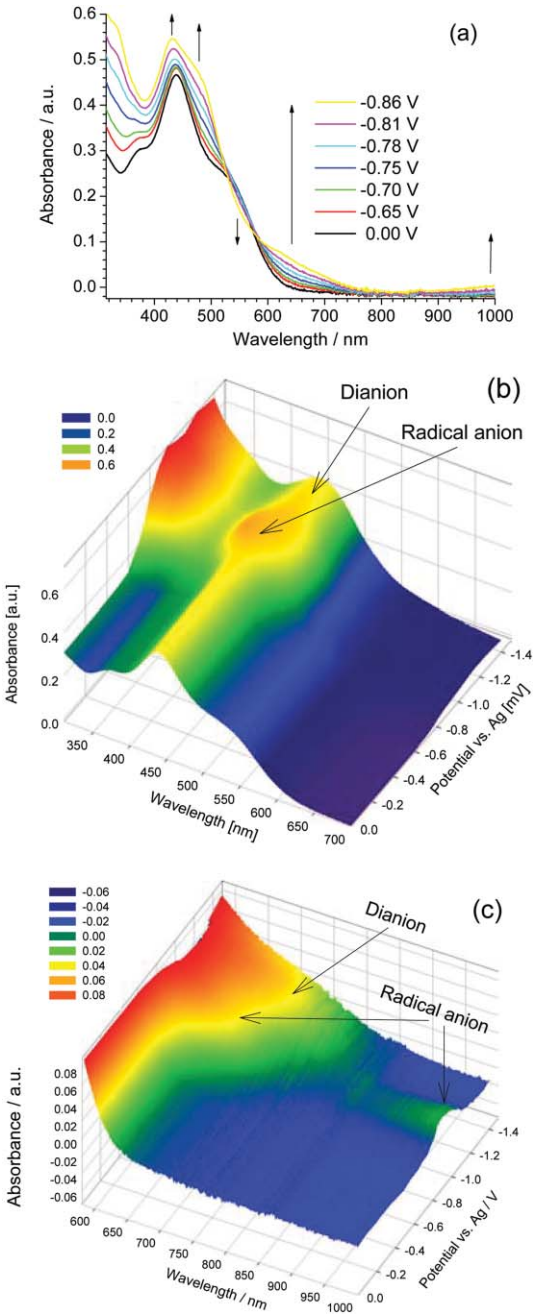

Fig. 2 Spectroelectrochemistry of **3** in benzonitrile, 0.1 M Bu_4NPF_6 (1 mm quartz cell, transmission mode, Pt grid working electrode, potentials are *vs.* Ag wire): a) reduction **3** → $\mathbf{3}^{2(\bullet-)}$; b) three dimensional representation of the SEC experiment in the potential range of 0 to −1.45 V; c) 3D representation of SEC experiment, magnified 600–1000 nm region.

studies are hindered by the irreversibility of the process as followed from CV experiments).

Absorption and photoinduced absorption spectroscopy

The optical absorption of **3**, see Fig. 5, shows an onset around 650 nm (E_g^{opt} = 1.9 eV) in toluene solution as well as in the solid state. This is slightly lower than the optical energy gap of

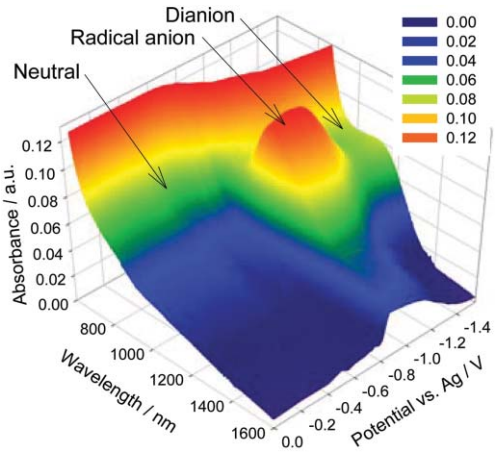

Fig. 3 3D representation of SEC experiment of **3** in benzonitrile, 0.1 M Bu_4NPF_6 at high concentration in potential range of 0 to −1.55 V (1 mm quartz cell, transmission mode, Pt grid working electrode, potentials are vs. Ag wire); NIR region has been shown.

the bare sexithiophene α-6T (E_g^{opt} = 2.1 eV from the onset)[35] and is complicated by the intramolecular charge transfer band of the donor–acceptor units (the ICT band for the terthiophene **15a** is clearly distinguishable and has a maximum at 532 nm). The electrochemical energy gap (E_g^{CV} = 1.5 eV, estimated from onsets of reduction and oxidation processes in the CV experiment, see Fig. 1) of compound **3** is significantly lower than the optical value, showing the diad character of the molecule (longest wavelength in **3** is due to ICT from the dithiole donor ring on to the acceptor fluorene moiety,[14,19,32] whereas the lowest oxidation potential arises from the sexithiophene conjugated chain). The photoluminescence shows a weak single peak around 620 nm in toluene solution, which is bathochromically shifted to 700 nm in the solid state (Fig. 5).

Photoinduced absorption (PIA) was measured on a home made setup in a liquid N_2 bath cryostat. The sample was excited by a modulated 476 nm line of an Ar^+ laser. Changes in the transmission dT of a tungsten lamp were detected with a Si/InGaAsSb sandwich detector and measured with a lock-in amplifier. dT was normalized to the white light transmission T, giving the PIA = −dT/T.

The PIA spectrum of **3**, Fig. 6, shows a broad peak between 0.9 and 1.9 eV with a plateau between 1.2 and 1.5 eV and a shoulder at 1.0 eV. Additionally, an emerging PIA feature for small probe energies is observed. Fig. 7 shows the expansion of the PIA for the NIR-MIR with a PIA peak around 0.4 eV and infrared active vibration (IRAV) bands in the MIR. The IRAV bands are a clear indication of charged species. The PIA at 0.4 eV might be assigned to the cation absorption of **3**.

The modulation frequency dependences at various probe energies are shown in Fig. 8. The PIA at 1.1 eV and 1.38 eV shows different modulation frequency dependences. Therefore, it is concluded that the broad absorption in the VIS-NIR originates from more than one photoexcited species. The shoulder at 1.1 eV shows the weakest dependence on the modulation frequency, indicating the shortest lifetimes. Fitting of the in-phase component (X) results in a lifetime of τ = 0.07 ms and a distribution factor of α = 0.40. The measured

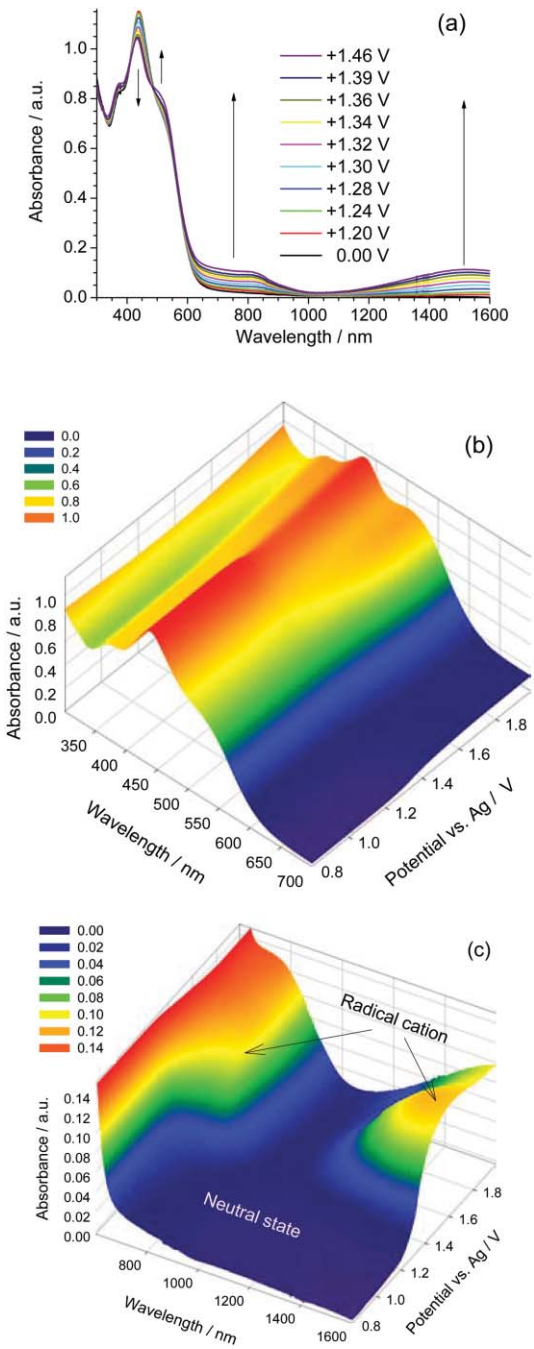

Fig. 4 SEC of **3** in benzonitrile, 0.1 M Bu_4NPF_6 (1 mm quartz cell, transmission mode, Pt grid working electrode, potentials are vs. Ag wire): a) oxidation **3** → **3**$^{\bullet+}$; b) 3D representation of the SEC experiment in potential range of +0.8 to +2.0 V, visible region; c) 3D representation of SEC experiment, NIR region.

range for the out-of-phase signal (Y) as well as the dependences at 0.62 and at 1.1 eV could not be fitted by any modulation frequency model. Fig. 9 shows the excitation intensity dependence at various probe energies. The signals are fitted by a power law and scale with $k \approx 1$. Such a dependence indicates first order kinetic recombination behaviour. This strongly indicates intramolecular photoexcited species.

In order to find out more information concerning the cation species of **3**, a blend with fullerene derivative [6,6]-phenyl-C_{61} butyric acid methyl ester (PCBM) as a strong electron acceptor was investigated ($E_{1/2}^{red1} = -0.69$ V *vs.* Ag wire).[36] The PIA spectrum shows peaks at 1.47 eV with a shoulder around 1.7 eV and at 0.7 eV (*cf.* with SEC experiments on generation of **3**$^{\bullet+}$, Fig. 4). All peaks in the blend show quite similar

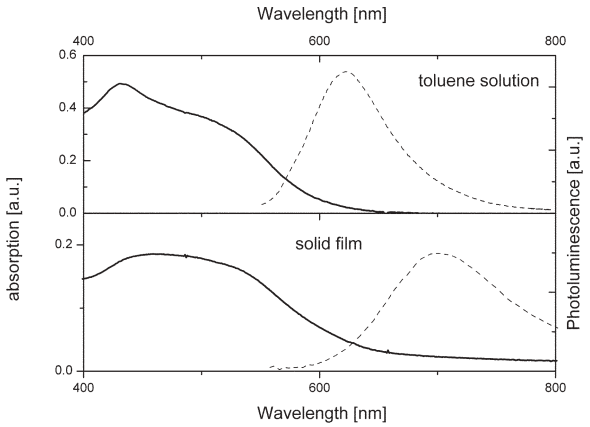

Fig. 5 Absorption (thick line) and photoluminescence spectra (dashed line) of **3** in a toluene solution (upper part) and as a solid film (lower part). Photoluminescence is excited at 500 nm for the solution and 476 nm for the thin film.

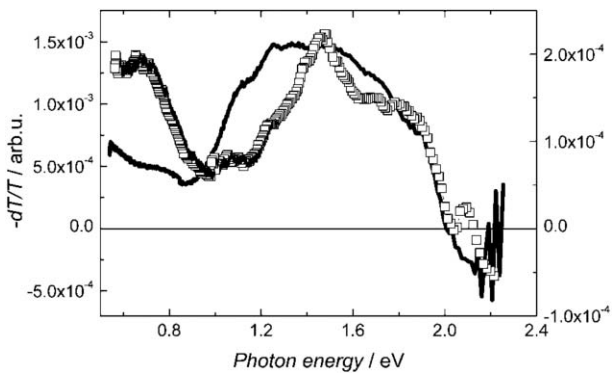

Fig. 6 PIA spectra of **3** thin film (full line, left axis) and a **3** : PCBM 1 : 1 blend film (open squares, right axis), spectra recorded at 80 K, excitation at 476 nm with 40 mW.

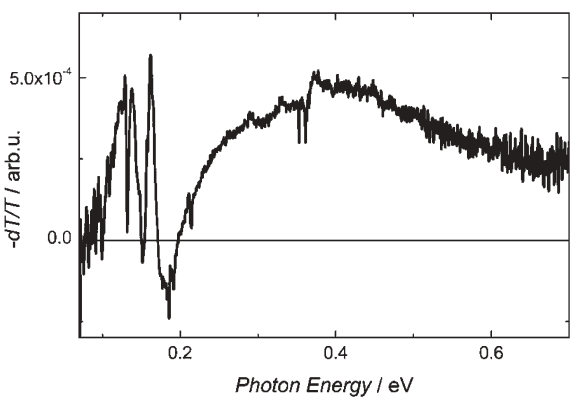

Fig. 7 PIA spectrum in the MIR-NIR infrared spectrum of a **3** film drop cast on KBr. Spectra are recorded at 80 K, 30 mW illumination at 476 nm. The PIA is obtained by subtracting the spectrum under illumination from the spectrum in the dark.

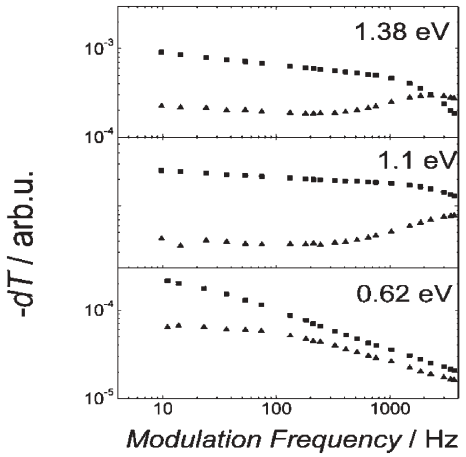

Fig. 8 Modulation frequency dependence of the PIA of **3** at 1.38 eV, 1.1 eV and 0.62 eV. No satisfactory fits could be obtained for these frequency dependences. For the 1.1 eV PIA, the in-phase component (squares) is fitted, giving a lifetime of 0.07 ms and a distribution factor of 0.4.

dependences on the modulation frequency at all investigated probe energies (see Fig. 10). None of the peaks could be fitted by a modulation dependence model. The excitation power dependence, Fig. 11, varies in a small range between $k = 0.55$ and $k = 0.65$, fitted by a power law. These results indicate bimolecular recombination as the dominant recombination mechanism. The recombination behaviour of the photoexcitations is quite different in the fullerene blend than for pristine **3**, leading us to conclude that different photophysical processes are involved.

For 6T cation, absorption peaks at 1.55 and 0.8 eV are reported.[37–40] These energies are quite comparable with the PIA of the **3** : PCBM blends. Although the two systems, 6T and **3**, are not directly comparable, it might be concluded that the positive charge is primarily located on the sexithiophene backbone. Furthermore, the PIA around 1.1 eV in **3** is quenched in the blend with PCBM. The lifetime of this feature

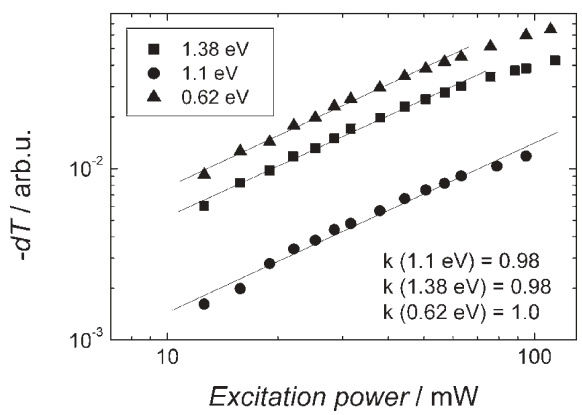

Fig. 9 Excitation power dependence of the PIA of **3** at 1.38 eV, 1.1 eV and 0.62 eV. Fits (thin line) are done by a power law. For high excitation intensities, saturation is observed. These points are not included into the fitting procedure.

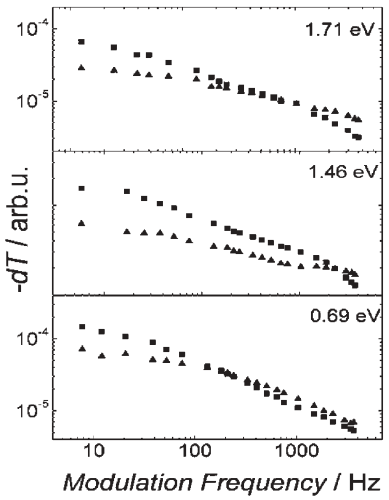

Fig. 10 Modulation frequency dependence of the PIA of **3** : PCBM 1 : 1 blend at 1.71 eV, 1.46 eV and 0.69 eV.

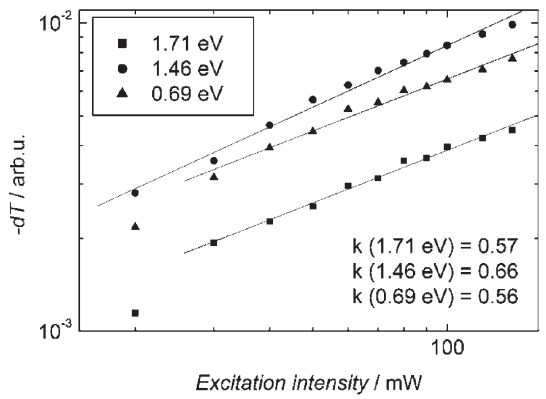

Fig. 11 Excitation power dependence of the PIA of **3** : PCBM 1 : 1 at 1.71.eV, 1.46 eV and 0.69 eV. Measurements were performed at 80 K with 37 Hz modulation. Fits are provided by a power law (thin line).

is found to be rather short and different to the positive charge. We assume therefore that this might be correlated to a triplet state or to a charge transfer state.

Photovoltaic devices

Photovoltaic devices were prepared for **3** : PCBM blends in a sandwich type geometry. ITO coated with PEDOT (Baytron PH) served as the positive contact, evaporated LiF/Al contact as the negative contact. The *I–V* characteristics and photocurrent spectrum are shown in Fig. 12. The device characteristics are mainly dominated by a low shunt resistance. Under illumination, the photoeffect is observed. The photocurrent spectrum matches the absorption spectrum well and shows its onset around 650 nm, coinciding with that of **3**. Devices show a photoeffect with a power conversion efficiency $\eta_e = 0.1\%$. The device performance is mainly limited by the low fill factor. The open circuit voltage of 0.64 V is comparable with other polythiophene fullerene bulk heterojunction devices.

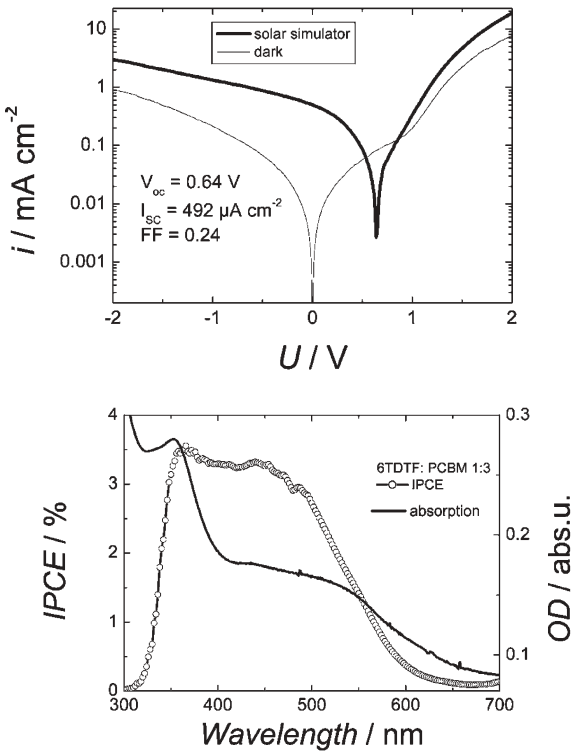

Fig. 12 *I–V* characteristics (above) under solar simulated light, 80 mW cm^{-2} and in the dark of a **3** : PCBM 1 : 3 blend, spin cast from chlorobenzene. Photocurrent spectrum in comparison with the absorption spectrum (below).

Conclusions

New routes towards fluorene functionalised oligothiophenes have been investigated. Within this theme, a new sexithiophene material with pendant 1,3-dithiol-2-ylidene-fluorene units has been prepared, characterised and used in a bulk heterojunction solar cell device. Whilst the power conversion efficiency is modest, the photocurrent spectrum indicates that the ICT process is also involved in the conversion of absorbed light to current. This sets a precedent for incorporating pendant donor–acceptor moieties into conjugated macromolecules for the purpose of improving light harvesting efficiency.

Acknowledgements

AK thanks the EPRSC (GR/T28379) and RB The Leverhulme Trust (F/00120/U) for funding.

References

1 C. J. Brabec, N. S. Sariciftci and J. C. Hummelen, *Adv. Funct. Mater.*, 2001, **11**, 15.
2 S. E. Shaheen, D. S. Ginley and G. E. Jabbour, *MRS Bull.*, 2005, **30**, 10.
3 J. L. Segura, N. Martín and D. M. Guldi, *Chem. Soc. Rev.*, 2005, **34**, 31.
4 M. C. Scharber, D. Mühlbacher, M. Koppe, P. Denk, C. Waldauf, A. J. Heeger and C. J. Brabec, *Adv. Mater.*, 2006, **18**, 789.
5 I. F. Perepichka, D. F. Perepichka, H. Meng and F. Wudl, *Adv. Mater.*, 2005, **19**, 2281.
6 M. R. Andersson, O. Thomas, W. Mammo, M. Svensson, M. Theander and O. Inganäs, *J. Mater. Chem.*, 1999, **9**, 1933.
7 A. Cirpan, A. A. Argun, C. R. G. Grenier, B. D. Reeves and J. R. Reynolds, *J. Mater. Chem.*, 2003, **13**, 2422.
8 G. Sonmez, *Chem. Commun.*, 2005, 5251.
9 C. D. Dimitrakopoulos and P. R. L. Malenfant, *Adv. Mater.*, 2002, **14**, 99.
10 Y. Sun, Y. Liu and D. Zhu, *J. Mater. Chem.*, 2005, **15**, 53.
11 M. M. Ling and Z. Bao, *Chem. Mater.*, 2004, **16**, 4824.
12 H. Tian, J. Wang, J. Shi, D. Yan, L. Wang, Y. Geng and F. Wang, *J. Mater. Chem.*, 2005, **15**, 3026.
13 H. Hoppe and N. S. Sariciftci, *J. Mater. Chem.*, 2006, **16**, 45.
14 P. J. Skabara, I. M. Serebryakov and I. F. Perepichka, *J. Chem. Soc., Perkin Trans. 2*, 1999, 505.
15 P. J. Skabara, I. M. Serebryakov and I. F. Perepichka, *Synth. Met.*, 1999, **102**, 1336.
16 P. J. Skabara, I. M. Serebryakov, I. F. Perepichka, N. S. Sariciftci, H. Neugebauer and A. Cravino, *Macromolecules*, 2001, **34**, 2232.
17 G. Sheldrick and M. Wyler, *Br. Pat.* 489 612, 1938.
18 Richardson-Merrel Inc., *Fr. Pat.* 2.211.235, 1974.
19 I. F. Perepichka, L. G. Kuz'mina, D. F. Perepichka, M. R. Bryce, L. M. Goldenberg, A. F. Popov and J. A. K. Howard, *J. Org. Chem.*, 1998, **63**, 6484.
20 A. Ferranti, A. Chiarini, L. Garuti, G. Giovanninetti and P. Brigidi, *Farmaco, Ed. Sci.*, 1982, **37**, 199.
21 O. Ishikawa, *Yuki Gosei Kagaku Kyokaishi*, 1959, **17**, 553 (*Chem. Abstr.*, 1960, 450).
22 B. D. Podoslov and D. S. Petrova, *Glas. Hem. Drus. Beograd*, 1966, **31**, 325 (*Chem. Abstr.*, 1969, **70**, 28692w).
23 G. W. Gray and A. Ibbotson, *J. Chem. Soc.*, 1957, 3228.
24 S. Berkowich, *Isr. J. Chem.*, 1963, **1**, 1.
25 J. G. Aston, J. D. Newkirk and D. M. Jenkins, *J. Am. Chem. Soc.*, 1943, **64**, 1413.
26 J. P. Guthrie and J. Cossar, *Can. J. Chem.*, 1990, **68**, 1640.
27 P. C. Putta and D. Mandal, *J. Indian Chem. Soc.*, 1956, **33**, 721.
28 F. E. Ray, M. R. Argus and C. P. Bart, *J. Org. Chem.*, 1947, **12**, 795.
29 N. Ueyama, S. Ueno, T. Sugawara, K. Tatsumi, A. Nakamura and N. Yasuoka, *J. Chem. Soc., Dalton Ttrans.*, 1991, 2723.
30 E. Sawicki, *J. Org. Chem.*, 1956, **21**, 271.
31 I. F. Perepichka, A. F. Popov, T. V. Orekhova, M. R. Bryce, A. M. Andrievskii, A. S. Batsanov, J. A. K. Howard and N. I. Sokolov, *J. Org. Chem.*, 2000, **65**, 3053.
32 D. D. Mysyk, I. F. Perepichka, D. F. Perepichka, M. R. Bryce, A. F. Popov, L. M. Goldenberg and A. J. Moore, *J. Org. Chem.*, 1999, **64**, 6937.
33 D. F. Perepichka, M. R. Bryce, E. J. L. McInnes and J. P. Zhao, *Org. Lett.*, 2001, **3**, 1431.
34 S. Amriou, I. F. Perepichka, A. S. Batsanov, M. R. Bryce, C. Rovira and J. Vidal-Gancedo, *Chem.–Eur. J.*, 2006, **12**, 5481.
35 P.A. Lane, X. Wei, Z. V. Vardeny, J. Poplawski, E. Ehrenfreund, M. Ibrahim and A. J. Frank, *Chem. Phys.*, 1996, **210**, 229.
36 C. J. Brabec, A. Cravino, D. Meissner, N. S. Sariciftci, T. Fromherz, M. T. Rispens, L. Sanchez and J. C. Hummelen, *Adv. Funct. Mater.*, 2001, **11**, 374.
37 R. A. J. Janssen, D. Moses and N. S. Sariciftci, *J. Chem. Phys.*, 1994, **101**, 9519.
38 P. A. Lane, M. Liess, X. Wei, J. Partee, J. Shinar, A. J. Frank and Z. V. Vardeny, *Chem. Phys.*, 1998, **227**, 57.
39 N. Yokounuma, Y. Furukawa, M. Tasumi, M. Kuroda and J. Nakayama, *Chem. Phys. Lett.*, 1996, **255**, 431.
40 J. A. E. H. van Haare, E. E. Havinga, J. L. J. van Dongen, R. A. J. Janssen, J. Cornil and J. L. Bredas, *Chem.–Eur. J.*, 1998, **4**, 1509.

